Mechanical Technology and Engineering Insights

www.mtei.reapress.com

Mech. Technol. Eng. Insights. Vol. 1, No. 1 (2024) 53–70.

Paper Type: Original Article

Comprehensive Study on the Effects of TIG Welding Parameters on the Microstructure and Mechanical Properties of Titanium Alloys: A Review

Agnes Essien Oboh[1,*], Michael Okon Bassey[2], Aniekan Essienubong Ikpe[3]

[1] Department of Mechanical and Aerospace Engineering University of Uyo, Uyo. Nigeria; agnesoboh@uniuyo.edu.ng.

[2] Department of Mechatronics Engineering, Akwa Ibom State Polytechnic, Nigeria; michael.bassey@akwaibompoly.edu.ng.

[3] Department of Mechanical Engineering Technology, Akwa Ibom State Polytechnic, Nigeria; aniekan.ikpe@akwaibompoly.edu.ng.

Citation:

Received: 16 March 2024 *Revised: 27 May 2024* *Accepted: 31 August 2024*	Oboh, A. E, & Bassey, M. O., Ikpe, A. S. (2024). Comprehensive study on the effects of TIG welding parameters on the microstructure and mechanical properties of titanium alloys: a review. *Mechanical technology and engineering insights, 1* (1), 53-70.

Abstract

Titanium alloys are widely used in various industries due to their excellent mechanical properties, corrosion resistance, and biocompatibility. However, the welding of titanium alloys poses challenges due to their high reactivity with oxygen and nitrogen, which can lead to the formation of brittle intermetallic compounds and porosity in the weld zone. The selection of appropriate TIG welding parameters is crucial to ensure the desired microstructure and mechanical properties in the welded joints. Therefore, there is a need for a comprehensive review of the effects of TIG welding parameters on the microstructure and mechanical properties of titanium alloys to provide guidelines for optimizing welding processes. The research methodology involved a systematic review of existing studies on TIG welding of titanium alloys. The research methodology involved a literature search of existing studies on TIG welding of titanium alloys using online databases. The selected studies were analyzed to identify the effects of welding parameters such as welding current, welding speed, and shielding gas flow rate on the microstructure and mechanical properties of titanium alloys. The analysis of the literature revealed that the selection of TIG welding parameters significantly influences the microstructure and mechanical properties of titanium alloys. Higher welding currents and slower welding speeds were found to increase the heat input, leading to larger grain sizes and reduced mechanical properties in the weld zone. On the other hand, lower welding currents and higher welding speeds resulted in finer microstructures and improved mechanical properties. Additionally, the use of appropriate shielding gas flow rates was found to minimize the formation of porosity and intermetallic compounds in the weld zone. The study provides valuable insights into the optimization of TIG welding processes parameters to achieve desired properties in the welded joints. Welding parameters should be selected carefully in order to control the heat input and minimize the formation of defects in the weld zone. Future research should focus on developing advanced welding techniques and process monitoring systems to further improve the quality of welded titanium alloys.

Keywords: Titanium alloys, Mechanical properties, TIG welding, Microstructure.

1 | Introduction

Two unique fabrication technologies that have revolutionized the manufacturing industry are Additive Manufacturing (AM) and TIG welding. TIG welding is a conventional method of fusing metals, whereas AM

Corresponding Author: agnesoboh@uniuyo.edu.ng

is a state-of-the-art process enabling layer-by-layer creation of complicated shapes. Since TIG welding can yield precise, high-quality welds with superior mechanical qualities, it is a widely used technique for connecting titanium alloys. Moreover, high integrity joints are necessary for titanium alloys used in manufactured aircraft structures in order to satisfy design specifications [1], [2]. The techniques of deploying TIG, Electron Beam Welding (EBW), Plasma Arc Welding (PAW), and Laser Beam Welding (LBW) may all produce high-quality fusion-welded connections in titanium alloys. Deep penetration with little overall heat input is made possible by the creation of a keyhole in high energy beam welding procedures because to the highly concentrated energy input.

Relatively low residual stresses and limited fusion and Heat Affected Zone (HAZ) microstructural changes result in welds with suitable fatigue and mechanical qualities. At significantly reduced capital costs, TIG and PAW give the possibility to produce welds that are on par with EBW or LBW in quality [3-6]. It has been demonstrated that TIG welds can have mechanical qualities that are similar to EBWs in both cast and wrought base materials, despite the fact that the increased heat input in arc welding methods results in broader weld zones with coarser microstructure. The low density (equivalent to 4.43 g/cm3 for Ti and 2.80 g/cm3 for Al) and strong mechanical properties (the average ultimate tensile strength is equal to 300 MPa for Al alloys and 1205 MPa for Ti alloys) are the distinguishing features of Titanium (Ti) and Aluminium (Al) alloys [7], [8]. In aircraft and automotive applications, where weight reduction is necessary along with excellent mechanical strength and corrosion resistance, Al–Ti dissimilar welds are of great importance. However, due to their dissimilar physical characteristics and the development of Intermetallic Phases (IMC), which cause cracks to occur during cooling and solidification, connecting Al/Ti alloys remains a challenging technological task. Reducing the thickness of the IMC layer at the interface and the quantity of IMC particles scattered across the aluminium Fused Zone (FZ) are necessary for the successful connecting of aluminium to titanium [9-11].

Actually, despite the attractiveness of intermetallic compounds based on the Ti–Al system–which exhibit strong properties at elevated temperatures–the growth of IMC results in limitations on the deformation modes that are accessible. Therefore, the presence of such particles is linked to a decrease in fracture toughness and ductility but an increase in strength. The chemical makeup of the weld zone, the welding process, microstructural components, and other factors can all have an impact on the mechanical and corrosion properties of the weld. Zhang et al. [12] and Long et al. [13] observed that the $\beta \rightarrow \alpha$ transformation's cooling rate-dependent process may alter the weld zone's shape. Increased cooling rate has the potential to alter weld cellular structure to a dendritic columnar shape. Furthermore, it has been said that epitaxial growth influences the grain size of Weld Metal (WM)via influencing the grain size of the HAZ [14], [15].

For instance, Ti-6Al-4V, a titanium alloy that is widely used, is characterized by its excellent reactivity to oxygen, low thermal conductivity, and relatively high strength at specific welding temperatures. Since titanium alloys maintain their increased strength and stability at comparatively high temperatures, they can be joined with other kinds of steels to achieve multifunctional applications. Ti-6Al-4V is an alpha-beta alloy; during the welding process, the microstructure's complexities are established in an effort to enhance the alloy's melting hardness and strength. As thermoplastic complex structures are used to withstand the static and fatigue pressures necessary for aerospace vehicles, their utilization is fast expanding and replacing that of their metallic and thermoset complex equivalents [16-19].

2 | TIG Welding Experimental Setup

One of the least stressful metals to weld with TIG is titanium, which may be done both manually and automatically. Metals can be joined together in the presence of an inert gas, such as argon, helium, or a combination of the two, by creating an arc between the workpiece and the tungsten alloy electrode, which shields the welded area from air contamination [20], [21]. Additionally, the gasses facilitate faster welding and electrode penetration using TIG, titanium alloys can be welded independently (without filler) or with the aid of filler wire [22], [23]. Detailed procedure for setting up a TIG welding experiment are as follows:

I. Safety precautions: before starting the TIG welding experiment, it is essential to ensure the safety of the operator and the surrounding environment. This includes wearing appropriate personal protective equipment such as welding gloves, helmet, and apron. Additionally, make sure the work area is well-ventilated to prevent exposure to harmful fumes.

II. Equipment set-up: the next step is to set up the TIG welding equipment. This includes the TIG welding machine, gas cylinder, tungsten electrode, filler rod, and workpiece. Make sure all equipment is in good working condition and properly connected.

III. Tungsten electrode Preparation: the tungsten electrode is a crucial component of TIG welding as it generates the arc. To prepare the tungsten electrode, grind the tip to a point using a dedicated tungsten grinder. The electrode should be sharpened to a fine point to ensure a stable arc during welding.

IV. Gas selection: TIG welding requires the use of a shielding gas to protect the weld pool from atmospheric contamination. Common shielding gases used in TIG welding include argon and helium. Select the appropriate gas based on the material being welded and set the flow rate according to the manufacturer's recommendations.

V. Welding parameters: before starting the welding process, set the welding parameters on the TIG welding machine. This includes adjusting the amperage, voltage, and travel speed based on the material thickness and type. Refer to the Welding Procedure Specification (WPS) for guidance on the correct parameters.

VI. Welding technique: once the equipment is set up and the welding parameters are adjusted, it is time to start the welding process. Hold the torch at a 15-20 degree angle to the workpiece and initiate the arc by striking the tungsten electrode against the workpiece. Maintain a consistent travel speed and filler rod feed rate to create a smooth and uniform weld bead.

VII. Post-welding inspection: after completing the welding process, inspect the weld for any defects such as cracks, porosity, or lack of fusion. Use non-destructive testing methods such as visual inspection, dye penetrant testing, or ultrasonic testing to ensure the weld meets the required quality standards.

TIG welding is a versatile welding technique that requires careful preparation and attention to detail. By following this procedure, TIG welding experiment can be successfully set-up and high-quality welds achieved. Remember to prioritize safety, adhere to welding parameters, and inspect the weld for quality assurance. TIG welding experimental setup for the purpose of welding a butt joint is depicted in *Fig. 1*.

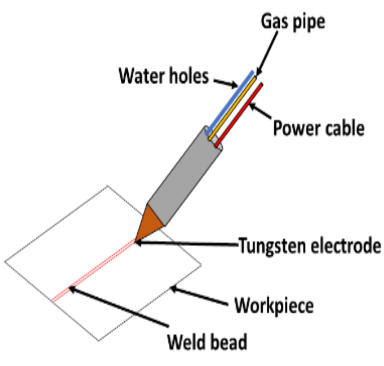

Fig. 1. Typical TIG welding Process showing automatic TIG welding machine [24].

2.1 | Preparation of Weld Joints for TIG Welding

The thickness of a metal can affects the joint preparation. For butt joint welding of Ti6Al4V alloys, plates thicker than 3 mm must first undergo edge preparation, which involves cutting a V-groove to allow for appropriate penetration. Rough-edged plates often result in more porosity in the weld [25]. To lessen thermal stress within the welded zone in plates thicker than 6 mm, the J groove is utilized rather than the V groove. In order to have a constant and good penetration, the J groove angle should be between 45° and 65°. This will also prevent distortions. When it is necessary to weld from both sides, a double V joint preparation may be used. The primary purpose of acid pickling is to thoroughly clean the metal surface in preparation for welding. It does this by eliminating oxygen and any other impurities from earlier processes [26], [27]. In order to achieve the best results when TIG welding, it is essential to properly prepare the weld joints. This process involves the following steps which must be applied carefully to ensure a strong and durable weld:

I. The first step in preparing a weld joint for TIG welding is to clean the surfaces that will be welded. This is crucial because any dirt, grease, or other contaminants on the surfaces can lead to poor weld quality. The surfaces can be cleaned using a wire brush, grinder, or chemical cleaner, depending on the material being welded.

II. After the surfaces are clean, the next step is to properly fit the pieces that will be welded together. It is important to ensure that the pieces are aligned correctly and that there is a small gap between them to allow for proper penetration of the weld. This can be achieved by using clamps or other tools to hold the pieces in place.

III. Once the pieces are properly fitted, the next step is to prepare the tungsten electrode. The electrode should be sharpened to a fine point using a grinder or dedicated electrode sharpener. The electrode should then be inserted into the TIG torch and secured in place.

IV. Before starting the welding process, it is important to set up the welding machine correctly. This includes selecting the appropriate welding current, gas flow rate, and other settings based on the material being welded. It is also important to ensure that the gas supply is connected and that the gas flow is adjusted to the correct level.

V. Once the welding machine is set up, the welding process can begin. The TIG torch should be held at the correct angle and distance from the workpiece, and the weld should be started by striking an arc between the electrode and the workpiece. The weld should be made by moving the torch in a controlled manner along the joint, ensuring proper penetration and fusion of the metal.

Proper preparation of weld joints is essential for achieving high-quality TIG welds. By following the process outlined above, welders can ensure that their welds are strong, durable, and free from defects. By taking the time to properly prepare the weld joints, welders can achieve the best results and produce high-quality welds that meet the highest standards of quality and craftsmanship.

2.2 | Description of TIG Welding of Titanium Alloys

Titanium is an element that possesses non-magnetic properties and sensible heat transfer [28]. Titanium alloys are widely used in various industries due to their excellent combination of high strength, low density, and corrosion resistance. When it comes to welding titanium alloys, Tungsten Inert Gas (TIG) welding is one of the most commonly used processes. TIG welding of titanium alloys involves the use of a non-consumable tungsten electrode to create the arc, while a shielding gas, typically argon, is used to protect the weld pool from atmospheric contamination. One of the key characteristics of titanium alloys is their high reactivity with oxygen, nitrogen, and hydrogen, which can lead to the formation of brittle intermetallic compounds and porosity in the weld. To prevent this, it is essential to maintain a high level of cleanliness in the welding environment and use proper shielding gas to protect the weld pool. Another important characteristic of titanium alloys during TIG welding is their high thermal conductivity, which can result in rapid heat dissipation and the formation of a narrow HAZ. This can lead to the risk of cracking in the weld, especially in thicker sections of the material. To mitigate this risk, it is crucial to control the heat input during welding and use proper preheating and post-weld heat treatment procedures.

In terms of behaviour, titanium alloys exhibit a tendency to form a protective oxide layer on the surface when exposed to air or high temperatures. This oxide layer can interfere with the formation of a sound weld, leading to poor penetration and incomplete fusion. To overcome this, it is necessary to remove the oxide layer using mechanical or chemical cleaning methods before welding. TIG welding of titanium alloys requires careful consideration of their unique characteristics and behaviours to ensure the production of high-quality welds. By understanding the reactivity, thermal conductivity, and oxide formation tendencies of titanium alloys, welders can effectively control the welding process and produce strong, defect-free welds. Proper cleaning, shielding gas selection, heat control, and post-weld treatments are essential steps in achieving successful TIG welding of titanium alloys. The physical properties of titanium compared to some competitor metals are presented in *Table 1* while the physical and mechanical properties of titanium alloy are shown in *Table 2*.

Table 1. Selected physical properties of Titanium and compared to some competitor metals.

	Ti	Al	Fe	Ni
Density [g/cm^3]	4.5	2.7	7.9	8.9
Melting point [degree Celsius]	1670	660	1538	1455
Thermal conductivity [W/mK]*	15-22	221-247	68-80	72-92
Elastic modulus [GPa]	115	72	215	200
Reactivity with oxygen	high +	high	low	low
Corrosion resistance	high +	high	low	medium
Metal price	high +	medium	low	high

Table 2. Physical and mechanical properties of Titanium.

1	Atomic number	22
2	Atomic weight	47.9
3	Atomic volume	10.6 weight/density
4	Covalent radius	0.132 nm
5	First ionization energy	661.5 MJ/(kJ mol)
6	Thermal neutron absorption cross section	560 fm^2/atmo
7	Crystal structure	close-packed, hexagonal≤1156 K body-centered, cubic>1156 K
8	Colour	Dark gray
9	Density	4510 kg/m^3
10	Melting point	1941 ± 285 K
11	Solidus/liquidus	1998 K
12	Boiling point	3533 K
13	Specific heat (at 298 K)	0.518 J/(kg K)
14	Thermal conductivity	21 W/(m K)
15	Heat of fusion	440 kJ/kg
16	Heat of vaporization	9.83 MJ/kg
17	Specific gravity	4.5
18	Hardness	HRB 70 to 74
19	Tensile strength	241 GPa
20	Modulus of elasticity	102.7 GPa
21	Young's modulus of elasticity	102.7 GPa
22	Poisson's ratio	0.41
23	Coefficient of friction	0.8 at 40 m/min 0.68 at 300 m/min
24	Specific resistance	0.554 μΩm
25	Coefficient of thermal expansion	8.64 x 10^{-4} K^{-1}
26	Electrical conductivity	3% IACS (Copper 100%)
27	Electrical resistivity	0.478 μΩm
28	Electronegativity	1.5 Pauling's
29	Temperature coefficient of electrical resistance	0.0026 K^{-1}
30	Magnetic susceptibility	1.25 x 10^{-6} μΩm
31	Machinability rating	40 %

3|Effects of TIG Welding Parameters on Microstructure of Titanium Alloys

Because TIG welding is widely used in industries, it is important to understand how different parameters affect the mechanical behaviour of Ti6Al4V alloy in order to reduce welding costs and obtain high-quality welds. Researchers have used a variety of statistical and experimental techniques to identify the parameters that can be compromised for another in order to have a high-quality weld with good mechanical properties. Taguchi method, Response Surface Methodology (RSM), etc. are common techniques used in optimizing these parameters, and Box-Behnken and Artificial Neural Network (ANN) are commonly used in prediction analysis of these parameters [29-31]. Additionally, current pulsing has a significant impact on the parameter selection for TIG welding. The main factors influencing the quality of TIG welds are peak current, background current, pulse frequency, and pulse on time [32]. When compared to an unpulsed frequency process, an increase in pulse frequency enhances the preceding β grain size within the FZ and influences the stress created in TIG welded Ti6Al4V alloy. The metal's thickness affects the joint preparation. For butt joint welding of Ti6Al4V alloys, plates thicker than 3 mm must first undergo edge preparation, which involves cutting a V-groove to allow for appropriate penetration [33], [17]. Rough-edged plates often result in more porosity in the weld.

To lessen thermal stress within the welded zone in plates thicker than 6 mm, the J groove is utilized rather than the V groove. In order to have a constant and good penetration, the J groove angle should be between 45° and 65°. This will also prevent distortions. If it's necessary to weld from both sides, a double V joint preparation may be used [34-36]. The presence of α' martensitic microstructure in the weld zone of Ti6Al4V alloy welded by TIG is expected to increase the microhardness of the alloy. They further observed that the pulsed current method of TIG welding exhibits better micro-hardness towards the FZ than the unpulsed mode, albeit with a significantly lower average hardness value. A higher pulse frequency results in a decrease in micro-hardness in the Fatigue Zone (FZ) because the previous β grains are finer than in the unpulsed process. It can also be associated with a high amount of residual stress.

Cheepu et al. [37] presented microstructures of TC4 Titanium Alloy welds at Fusion Zone (FZ) produced with the welding current of 80, 120, 150 and 160 A as shown in *Fig. 2a-2d*. The increase in heat input in the welds leads in the formation of larger grains especially at the welding current of 120 A. the presence of single enlarged grain in the FZ may be one of the reason to decrease in strength of the joints. When the welding current increased from 150 A, the microstructures showed different from the lower welding currents. The microstructures at higher welding current and speed are showed finer grains and with the less number of enlarged grains. Due to this, the welds achieved highest strength at the higher welding currents even though the variation in the welding speeds.

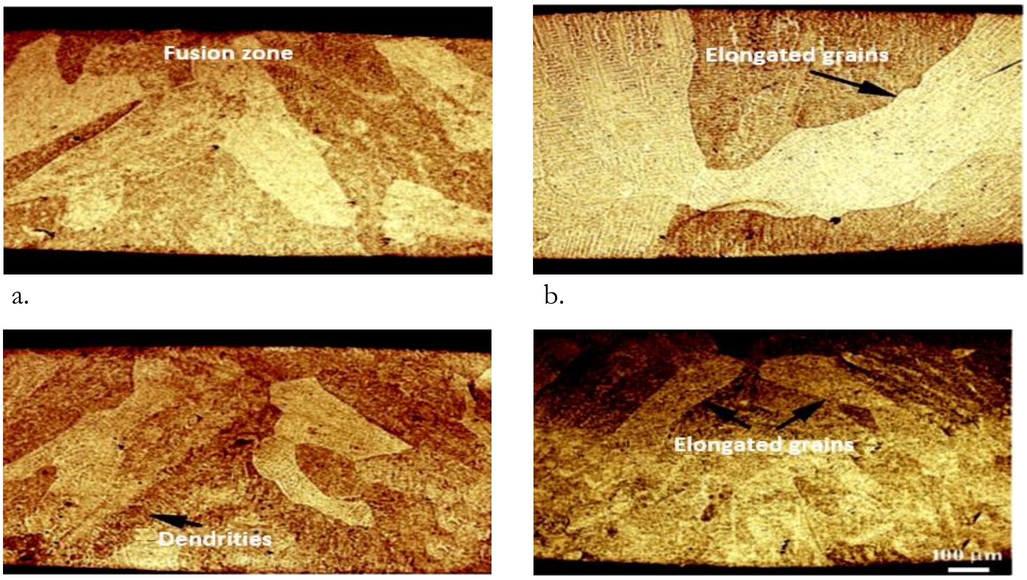

a. b.

c. d.

Fig. 2. Microstructures of TC4 titanium alloy welds at fusion zone produced with welding currents; a. 80 A, b. 120 A, c. 150 A, d. 160 A.

Fig. 3a-3b presented by Szwajka et al. [38] illustrates the microstructure of pure grade 1 titanium weld, showing a fine acicular structure and coarse grains under the influence of heat input due to welding temperature. It was observed that as the flow of the shielding gas decreases, the hardness of the weld material increased and its brittleness also increased. A similar trend related to the amount of gas flow was also noticeable for the tensile strength of the joints. Due to the lack of proper protection of the weld root by shielding gas, the WM was contaminated by elements from the surrounding atmosphere, which resulted in porosity of the WM (see *Fig. 3c*). It was observed that the number of pores in the weld on the side of the root increased as the shielding-gas flow rate decreased. *Fig. 3c* shows a cluster of pores in the weld made with the lowest shielding-gas flow rate.

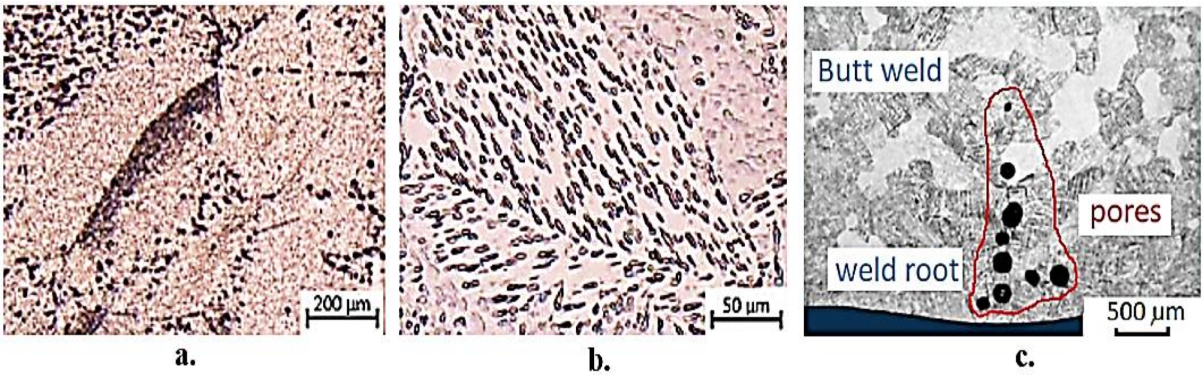

Fig. 3. Microstructure of commercially pure grade 1 titanium weld.

As seen in *Fig. 4*, a welded metal is made up of three components: the Base Metal (BM), the HAZ, and the FZ. The area that receives the most heat during welding is known as the flux zone, or WZ. This zone reaches the liquidus temperature before solidifying as a result of cooling. The high hardness in the region is mostly caused by the α' martensitic microstructure seen in the FZ. Comparable to the liquidus temperature, the HAZ in Ti6Al4V is also composed of α' martensitic microstructure, but it reaches a lower temperature-below the liquidus temperature mostly above the β transus temperature of 995°C. It can be observed that the α and β phases make up the BM [39-41].

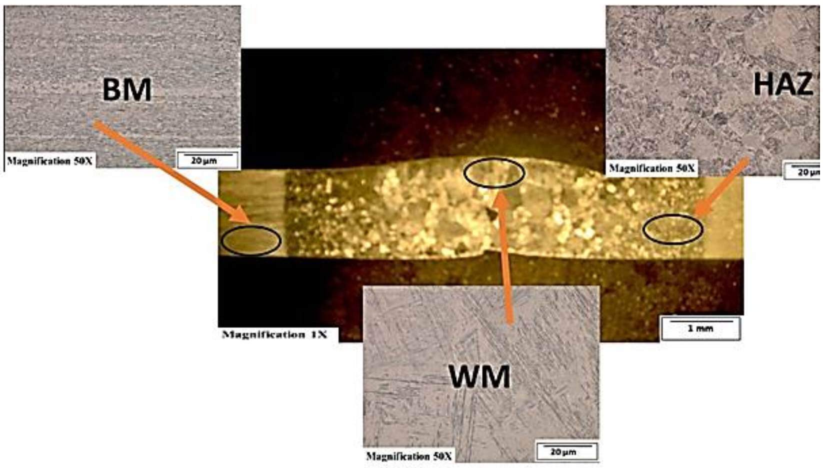

Fig. 3. Macrograph illustrating the three zones of TIG welded workpiece [22].

3.1 | Application of Titanium Alloys in Aviation Sector

Because of their high strength-to-weight ratio, low thermal expansion, resistance to embrittlement at low temperatures, good corrosion resistance, and heat resistance, titanium alloys are becoming more and more competitive materials. The aviation industry consumes the largest part of titanium [42], [43]. The applications of titanium in U.S recently are schematically showed in *Fig. 5*. Almost 84% of the titanium is used in the field related to the aviation industry. Titanium alloys are widely used to reduce fuel consumption [44] For instance, Airframes and engine components are increasingly made of Carbon Fibre Reinforced Plastic (CFRP) in an effort to reduce the amount of fuel that aeroplanes require. Similar to this, titanium's excellent compatibility with CFRP in terms of corrosiveness concerns and coefficient of thermal expansion has led to an increase in demand for it [45-48].

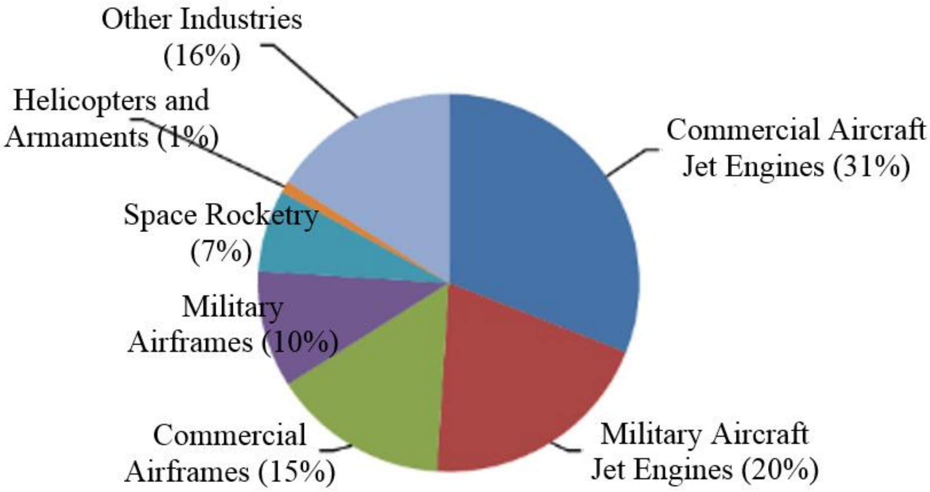

Fig. 5. Applications of titanium alloy (Ti-6A1-4V) in U.S [44].

Titanium alloys find application in gas turbine engines as well as air-frame constructions. Because of their superior mechanical qualities, which are related to their microstructures, metastable β titanium alloys are one of the essential parts used in the aviation sector [49]. Over the years, it has been able to draw the interest of researchers worldwide. *Table 1* illustrates the use of several titanium alloys in certain areas of the aviation sector.

Table 1. Application of specific titanium alloys in selected parts of aviation sector.

Systems and parts	Materials
Hydraulic tubing	Ti-3Al-2.5V [50]
Fan disks	Ti-6Al-2Sn-4Zr-6Mo [43]
Forgings, fasteners	Ti-5Al-5Mo-5V-3Cr; Ti-3Al-8V-6Zr-4Mo-4Zr [43]
Springs	Ti-3Al-8V-6Cr-4Mo-4Zr; Ti-15V-3Cr-3Al-3Sn [51]
Exhaust system	Ti-35V-15 Cr [43]
Wing box	Ti-6Al-4V [43]
Landing gear	Ti-10V-2Fe-3Al [51], [43]
	Ti-5Al-5Mo-5V-3Cr [45]
Windows frames	Ti-6Al-4V [43]
Mid-fuselage bulkhead	Ti-6Al-2Zr-2Sn-2Mo-2Cr-0.25Si [52]
Compressor stators	Ti-35V-15Cr [53]

3.2 | Effect of Textures on Titanium Alloys

Recrystallisation and deformation might affect the textures. Every crystal has a varied slip of dislocation and is subjected to varying amounts of stress. The grains will rotate, harden, and distort as a result of it. Anisotropic behaviour in terms of strength, Young's modulus, and elongations can be caused by the texturing. The critical value of the shear stress for slip on the crystallographic plane can be attributed to the cause of this situation. Grains differ in their Schmid factors, which have an impact on how slip systems activate. In other words, the various values of the Schmid factor in each direction define the plastic anisotropy of polycrystals [54-57]. Texture control after severe deformation allows for the control of anisotropy through temperature and duration of solution treatment. *Fig. 6* illustrates how an Elasto-Viscoplastic Self-Consistent (EVPSC) model with various Zener factors can compute the impact of texture components on Young's modulus [58], [59].

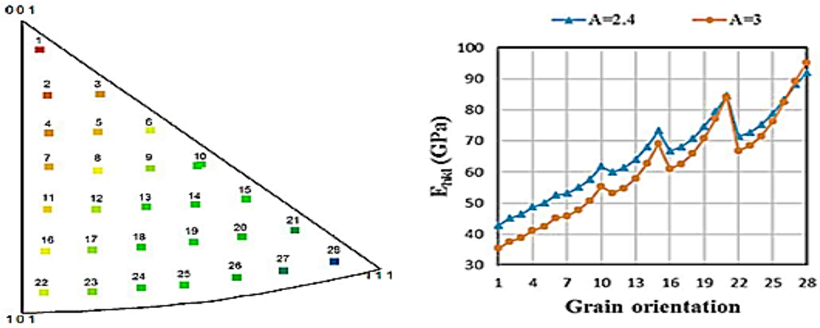

Fig. 6. Young's modulus parallel to the tensile axis of single crystal in 28 orientations obtained from two different β-phase single Crystal Elastic Constants (SEC); a: The numbering of 28 orientations of single crystals, b: Youngs modulus of these 28 orientations [58].

Generally, the two fibres that make up the common texture of titanium alloy after recrystallisation are the α- and γ-fibers. Stereographic projection of orientation relationship from β to α transformation is shown in *Fig. 7*. A class of textures known as α-fiber has a h110i axis that runs parallel to the direction of rolling. This fiber's principal constituents are {001}h110i, {112}h110i, and {111}h110i. A collection of textures known as γ-fiber have their h111i axis parallel to the normal direction of the sheet. This fiber's principal constituents are {111}h110i, {111}h112i, and {111}h123i [60], [61]. One easy way to convey textures is with the Orientation Distribution Function (ODF). Texture component analysis has made extensive use of Euler space. The texture components in Euler space are frequently collected into a few distinct fibers during the processing of metallic materials. When analyzing the texture, it is more effective to plot the orientation distribution's intensity along these fibers. The most studied α-, γ-, and ε-fibers are for bcc metals [62-64].

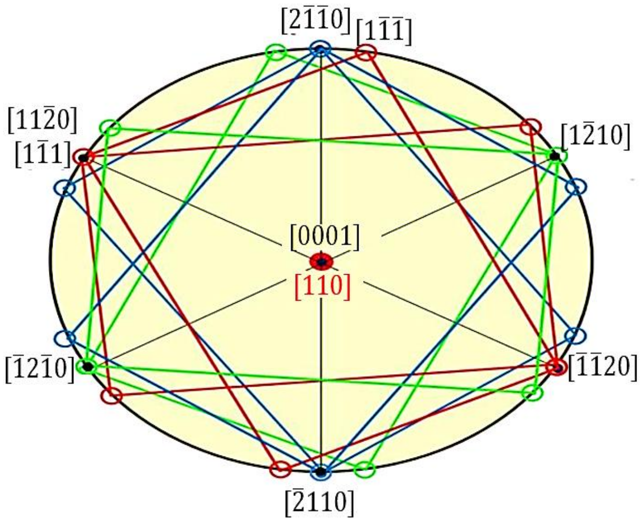

Fig. 7. Stereographic projection of orientation relationship from β to α transformation [65].

4 | Tensile and Fatigue Properties

The specific phase morphology has a significant impact on the mechanical properties of two-phase titanium alloys. The most important factors affecting alloys with α-lamellar microstructure are the colony diameter and the thickness of the lamellae. A higher yield stress is the outcome of microstructure refinement (see *Fig. 8a*). If the martensitic phase is absent, the rise in yield stress is, however, moderate. First, as the cooling rate increases, tensile elongation increases (see *Fig. 8b*). However, the ductility curve decreases after reaching its maximum. This behaviour was previously documented and linked to the transition of the fracture mode at main β grain boundaries from ductile transcrystalline fracture at low cooling rates to ductile intercrystalline fracture along continuous α phase layers.

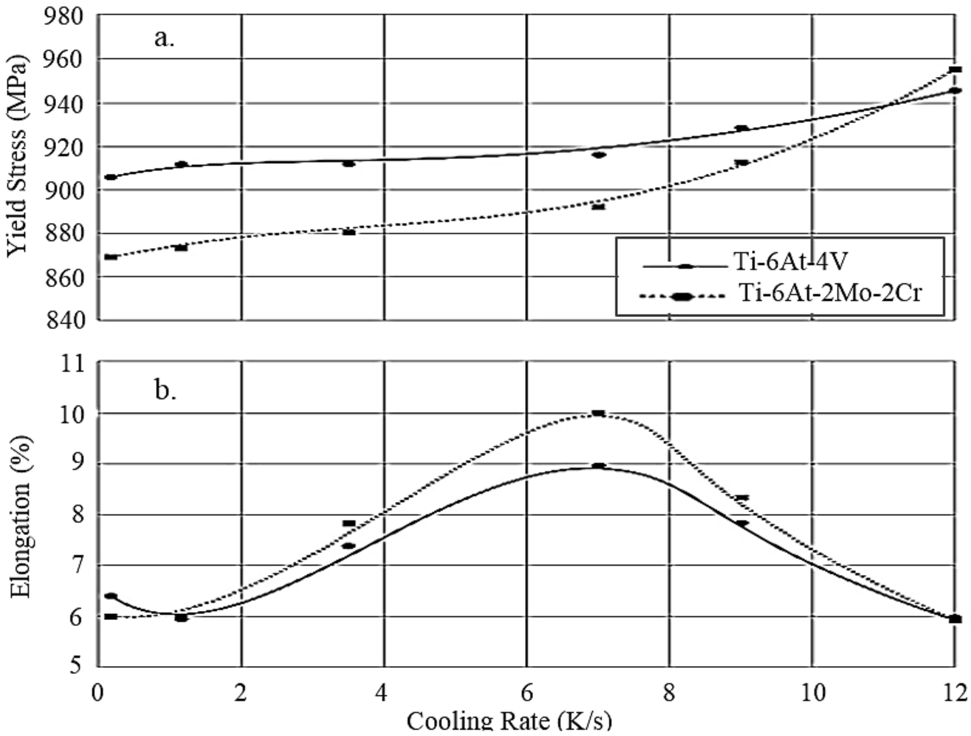

Fig. 8a-8b. Yield stress and tensile elongation dependence on the cooling rate from β-phase range for selected titanium alloys.

Since the size of the colonies of α lamellae with the same crystallographic orientation is a measure of effective slip length, it has a major impact on the alloy's mechanical properties. The measurement of colony size becomes considerably more challenging with the move to the "basket weave" type of microstructure. Consequently, the α-lamellae thickness was considered as a quantitative parameter to illustrate how microstructure refinement affects mechanical properties [51], [43].

4.1 | Fatigue Life Prediction on Titanium Alloy

Depending on the conditions of their use, lightweight, high-strength titanium alloys with excellent specific strengths at temperatures as high as 500-600°C are used for automotive engine parts, exhaust systems, and structural members of aircraft. They also need to have a variety of properties, including strength, fatigue strength, fracture toughness, creep resistance, and resistance to oxidation. The aircraft industry has been the primary focus of research into the effects of micro-structure, texture, chemical compositions, and other factors on the fatigue properties of titanium alloys. The development of fail-safe and damage-tolerant design has increased reliability [43], [51], [66].

The fatigue life of the weld is significantly impacted by the welding residual stresses; these stresses can regulate the fatigue life by either nucleating the crack or increasing the fracture grain size. The life of spot weld specimens is primarily determined by the type of specimen, feasible load amplitudes, diameter, and thickness specifications for the weld shape, as fatigue cracks may arise due to plastic strain at the notches. After the coiled tubes were welded together, it was discovered that the high-strength tubing had longer fatigue lifetimes than the low-strength tubing, which had higher internal pressures. Tensile testing is necessary to evaluate the elastic characteristics because the endurance limit can vary [67], [68]. When calculating the fatigue life to fracture initiation, parameters such as grain size and stress concentrations are taken into account. The bending fatigue results of the weld material can be determined by calculating the ratios at which the energy is unconstrained and the threshold stress intensity concentration factors that are associated with the voids. The relationship between the fatigue size and the associated fatigue life is important for fatigue design and its estimation, and if fatigue damage happens during the process, it causes the gap to form between the two phases [69], [43].

When the fracture begins to proliferate, the fatigue cyclic life may be prolonged. Consequently, the stress-strain characteristics may have a significant impact on the induced geometry, which may significantly slow down the pace of crack propagation.

When low cycle fatigue occurs, an irregular specimen's fatigue life initially equates to the regular specimen's total fatigue life when both specimens are subject to the same stress and strain range parameters. It is shown in spot-welded constructions that the fatigue life of a material reduces with increasing stresses, but increases with increasing spot-welded diameter [70], [69]. The internal surface was identified as the site of fatigue fracture start in the fatigue study, and *Fig. 9* shows the schematic depiction. It was also discovered that the high temperature environment and the air environment differed in the fatigue resistance of TI tubes.

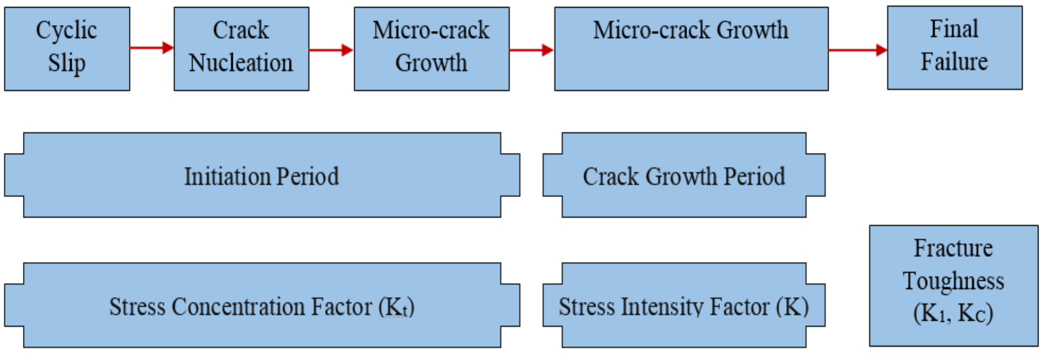

Fig. 9. Fatigue life phase and factors [15].

5 | Effect on Welding Current and Voltage on Titanium

The welding current may be computed using the Hall-Effect current sensor, and it is discovered that the current is encircled at the contact tip of the welding pistol and fixture, from which the arc voltage can also be computed. The process inputs (current and voltage) can be changed by comparing the variables (temperature, resistance, reflection, velocity) with the material responses. The arc voltage can protect the arc length and WM characteristics; as the arc voltage rises, the arc length rises as well, resulting in a broader bead thickness [32], [71]. Within a specific range, increasing the welding current during the TIG welding process results in increased heat and thermal force exerted on the workpiece. Consequently, as the current increases, the thermal heat also increases, leading to slight increase in voltage [72], [73].

The experiment on the arc and metal efficiency was carried out using the various processes, and it was determined that the arc efficiency has not varied much within a particular process for the choice of current explored. In the case of gas metal arc welding, droplet size measurement revealed that the droplet size falls and begins to deviate from the computed standards as the current increases. The changes in the weakening contact tube may be covered by the variations in the current for the steady range of voltage power source introduced by the Contact Tube-to-Work Distance (CTWD). Two areas arise in the TIG technique, which at first boost the tensile characteristics and then decline due to the grain size refinement, regardless of modifications in the base current and pulse-on-time [71-75].

6 | Porosity Variation and its Cracking on Welding of Titanium Alloys

The term "porosity" or "pores" usually refers to the cavities present in the welded metal. It is known that the WM porosity of a titanium alloy is formed from the base of the weld pool. The titanium welding procedure rounds up the pores, which is associated with the evolution of gas. The pore cracking process has properties on crack initiation and propagation according on the loading circumstances. The organization of the weld porosity happens as a result of imperfections caused by oil, grease, and dirt on the weld pieces outside [76-79]. The weld bead geometry has the most control over the fatigue act of the joint in the microstructure in the WM area. Large levels of porosity are introduced into the FZ section as a result of improper laser welding conditions, and it is demonstrated that the porosity is close to the tapering FZ of the defective penetration welds. Pore cracking starts at the pores before leak pathways form, and leaks are predicted to occur from cracks with deeply buried large pores. Smaller weld pools at low heat input stages enable faster solidification, which in turn causes porosity arrangement because the bubbles that were previously unable to escape are trapped by the solidification process. Three phases-bubble formation, expansion, and escape define the closure of porosity development [79-82].

7 | Effect of Residual Stress on Welding Titanium Alloys

In the weld, the transverse residual stresses are tensile, while the exterior areas experience compressive residual stresses to balance the stresses. The maximum tensile residual stress (200 MPa) is located at the weld center and represents approximately 25% of the base substance's yield strength when the material in a friction stir welding process is exposed to enough air cooling roughly 760 degrees Celsius for 45 minutes in an argon atmosphere-residual tension can be reduced [83], [84]. High tensile residual stresses during the welding process encourage fracture in the weldment, while compressive residual stresses in the base shield connect with the deformation periodically and may reduce the buckling strength.

The fatigue strength of a material with high tensile residual stresses varies little, but it can be considerably developed by an appropriate compressive residual stress. Based on the morphology of titanium alloys, friction welds can lead to various problems with structural integrity. One of these is when the titanium has reduced thermal conductivity; in this case, the friction welds are inherently linked to high residual stress [85], [86]. The transverse and longitudinal residual stress standards decreased by the side of the welding direction, respectively, according to the unique effects of the Deep Cryogenic Treatment (DCT) on the residual stress of EBW of Ti-6Al-4V joints. In conclusion, the residual stresses are produced by two processes, according to the linear friction welds. The material's plastic deformation at high temperatures is the primary cause. The second reason is the difference in the substance's thermal extension and decrease during heating and cooling, which causes thermally induced strain [87-89]. Through wear and tear, environmental deterioration, and creep, residual pressures can exacerbate the damage. Because the weld material heats up and expands during the welding process, compressive yielding happens right around the molten material. On the other hand, tensile residual stress is created in the longitudinal direction of the weld during cooling and shrinkage of the metal. Due to the specimen's high temperature preheating during the application of the stress relief behaviour, in laser gas nitriding, the specimen reduces its residual stress value after the nitriding procedure. In most circumstances, it is possible to determine the precise criteria for a crack under combined load by selecting a fracture under tensile residual stress; nevertheless, the external load scenarios should have different requirements. It was discovered that the laser-welded joints had superior super plasticity at low strain rates. Peak stress of the material at the weld zone was shown to decrease with rising temperature and lowering strain rate, although the peak stress remained higher than that of the parent material [90-92].

8 | Conclusion

In this research, the findings from conventional studies comparatively underscore the importance of understanding the complex interplay between TIG welding parameters, microstructure, and mechanical properties of titanium alloys. The review of existing literature has shown that the choice of welding parameters, such as welding current, welding speed, and shielding gas flow rate, can have a significant impact on the microstructure and mechanical properties of titanium alloys. For example, higher welding currents have been found to result in larger grain sizes and reduced mechanical properties, while higher welding speeds have been associated with finer grain sizes and improved mechanical properties. Furthermore, the review has highlighted the importance of optimizing welding parameters to achieve the desired balance between microstructure and mechanical properties. By carefully selecting the appropriate welding parameters, it is possible to tailor the microstructure of titanium alloys to meet specific performance requirements, such as improved strength, ductility, and fatigue resistance. By leveraging this knowledge, researchers and engineers can develop more efficient and effective welding processes for titanium alloys, ultimately leading to enhanced performance and reliability in a wide range of applications.

Based on the findings from conventional studies, the following recommendations are suggested in order to improve the overall performance of titanium alloy welds.

I. It is important to carefully control the welding parameters, such as welding current, welding speed, and shielding gas flow rate, to ensure the formation of a sound weld with minimal defects. Studies have shown that variations in these parameters can significantly affect the microstructure and mechanical properties of the weld, so it is crucial to establish optimal settings for each parameter based on the specific alloy being welded.

II. Pre-weld and post-weld heat treatments should be considered to refine the microstructure of the weld and enhance its mechanical properties. Heat treatments can help to eliminate residual stresses, improve the distribution of alloying elements, and enhance the overall strength and toughness of the weld. By carefully selecting the appropriate heat treatment process, the performance of titanium alloy welds can be significantly improved.

III. The use of filler materials with compatible composition and properties is essential for achieving high-quality welds in titanium alloys. Studies have shown that the selection of the right filler material can have a significant impact on the microstructure and mechanical properties of the weld, so it is important to carefully consider the compatibility of the filler material with the BM to ensure a strong and durable weld.

By carefully controlling welding parameters, utilizing appropriate heat treatments, and selecting compatible filler materials, the performance of titanium alloy welds can be optimized and their mechanical properties enhanced. Implementing these recommendations can help to improve the overall quality and reliability of titanium alloy welds in various industrial applications

References

[1] Karayel, E., & Bozkurt, Y. (2020). Additive manufacturing method and different welding applications. *Journal of materials research and technology*, *9*(5), 11424–11438. DOI: 10.1016/j.jmrt.2020.08.039

[2] Zhai, X., Jin, L., & Jiang, J. (2022). A survey of additive manufacturing reviews. *Materials science in additive manufacturin*, *1*(4), 21. DOI: 10.18063/msam.v1i4.21

[3] Tolvanen, S., Pederson, R., & Klement, U. (2024). Microstructure and mechanical properties of Ti-6Al-4V welds produced with different processes. *Materials*, *17*(4), 782. DOI: 10.3390/ma17040782

[4] Tolvanen, S. (2016). Microstructure and mechanical properties of ti-6al-4v welds produced with different processes. [Thesis]. https://acesse.dev/ZhhMd

[5] Junaid, M., Rahman, K., Khan, F. N., Bakhsh, N., & Baig, M. N. (2019). Comparison of microstructure, mechanical properties, and residual stresses in tungsten inert gas, laser, and electron beam welding of Ti--5Al-2.5 Sn titanium alloy. *Proceedings of the institution of mechanical engineers, part l: journal of materials: design and applications*, *233*(7), 1336–1351. DOI: 10.1177/1464420717748345

[6] Sonar, T., Ivanov, M., Trofimov, E., Tingaev, A., & Suleymanova, I. (2024). A comprehensive review on fusion welding of high entropy alloys – Processing, microstructural evolution and mechanical properties of joints. *International journal of lightweight materials and manufacture*, *7*(1), 122–183. DOI: 10.1016/j.ijlmm.2023.06.003

[7] Li, H., Zou, J., Yao, J., & Peng, H. (2017). The effect of TIG welding techniques on microstructure, properties and porosity of the welded joint of 2219 aluminum alloy. *Journal of alloys and compounds*, *727*, 531–539. DOI: 10.1016/j.jallcom.2017.08.157

[8] Zhang, D., Wang, G., Wu, A., Zhao, Y., Li, Q., Liu, X., … Zhang, Z. (2019). Study on the inconsistency in mechanical properties of 2219 aluminium alloy TIG-welded joints. *Journal of alloys and compounds*, *777*(10), 1044–1053. DOI: 10.1016/j.jallcom.2018.10.182

[9] Li, J., Dong, R., Kou, H., Fan, J., Zhu, B., & Tang, B. (2020). Texture evolution and the recrystallization behavior in a near β titanium alloy Ti-7333 during the hot-rolling process. *Materials characterization*, *159*, 109999. DOI: 10.1016/j.matchar.2019.109999

[10] Karim, M. A., & Park, Y. D. (2020). A review on welding of dissimilar metals in car body manufacturing. *Journal of welding and joining*, *38*(1), 8–23. DOI: 10.5781/JWJ.2020.38.1.1

[11] Elmi Hosseini, S. R., Fernandes, F. A. O., Pereira, A. B., & Li, Z. (2022). Welding of dissimilar materials in aerospace systems. In Kucshan, M. C. … Sofuouglu, M. A. (Eds.), *Materials, structures and manufacturing for aircraft* (pp. 317–344). Cham: Springer International Publishing. DOI: 10.1007/978-3-030-91873-6_13

[12] Zhang, K., He, C., Liu, D., Yan, C., Niu, H., Yang, Z., & Bao, Y. (2022). Effect of heat input on microstructure and tensile properties of laser welded Ti–3Al–6Mo–2Fe–2Zr alloy joint. *Journal of materials research and technology*, *17*, 1652–1661. DOI: 10.1016/j.jmrt.2022.01.089

[13] Long, J., Zhang, L. J., Ning, J., Zhang, L. L., Wang, X., Li, S., & Na, S. J. (2021). Effects of post-weld heat treatment on microstructures and properties of laser welded joints of new high-strength Ti-55531 alloy. *Journal of manufacturing processes*, *64*, 1329–1335. DOI: 10.1016/j.jmapro.2021.02.042

[14] Paul, A. R., Mukherjee, M., & Singh, D. (2022). A critical review on the properties of intermetallic compounds and their application in the modern manufacturing. *Crystal research and technology*, *57*(3), 2100159. DOI: 10.1002/crat.202100159

[15] Kumar, B., Kebede, D., & Bag, S. (2018). Microstructure evolution in thin sheet laser welding of titanium alloy. *International journal of mechatronics and manufacturing systems*, *11*(2–3), 203–229. DOI: 10.1504/IJMMS.2018.092875

[16] Wei, G., Tan, M., Attarilar, S., Li, J., Uglov, V. V., Wang, B., … Wang, L. (2023). An overview of surface modification, a way toward fabrication of nascent biomedical Ti-6Al-4V alloys. *Journal of materials research and technology*, *24*, 5896–5921. DOI: 10.1016/j.jmrt.2023.04.046

[17] Xu, J., Zhang, J., Shi, Y., Tang, J., Huang, D., Yan, M., & Dargusch, M. S. (2022). Surface modification of biomedical Ti and Ti alloys: a review on current advances. *Materials*, *15*(5), 1749. DOI: 10.3390/ma15051749

[18] Senopati, G., Rahman Rashid, R. A., Kartika, I., & Palanisamy, S. (2023). Recent development of low-cost β-Ti alloys for biomedical applications: a review. *Metals*, *13*(2), 194. DOI: 10.3390/met13020194

[19] Bassey, M., Offiong, U., & Ikpe, A. (2023). Finite element simulation for thermo-mechanical transient behavior of mild steel plate agglutinated by gas tungsten arc welding (GTAW) technique. *Journal of materials engineering, structures and computation*, *2*(3), 549–559. DOI: 10.5281/zenodo.8306756

[20] Ikpe, A. E., & Bassey, M. O. (2023). Modelling and simulation of transient thermal stress distribution across AISI 1018 flat plates at variable welding temperature regime. *Journal of materials engineering, structures and computation*, *2*(3). https://journals.nipes.org/index.php/jmsc/article/view/672

[21] Omoniyi, P. O., Mahamood, R. M., Jen, T. C., & Akinlabi, E. T. (2021). An overview of TIG welding of Ti6Al4V: recent developments. *Journal of composite & advanced materials/revue des composites et des matériaux avancés*, *31*(5), 265–274. DOI: 10.18280/rcma.310501

[22] Vijayakumar, V., Sonar, T., Venkatesan, S., Negemiya, A., & Ivanov, M. (2024). Influence of IP-TIG welding parameters on weld bead geometry, tensile properties, and microstructure of Ti6Al4V alloy joints. *Materials testing*, *66*(9), 1464. DOI: 10.1515/mt-2023-0237

[23] Devore, J. L., Berk, K. N., & Carlton, M. A. (2021). Statistical intervals based on a single sample. In *Modern mathematical statistics with applications* (pp. 451–499). Springer. DOI: 10.1007/978-3-030-55156-8_8

[24] Chang, J., Cao, R., & Yan, Y. (2019). The joining behavior of titanium and Q235 steel joined by cold metal transfer joining technology. *Materials*, *12*(15), 2413. DOI: 10.3390/ma12152413

[25] Andersson, J. (2020). Welding metallurgy and weldability of superalloys. *Metals*, 10(1), 143. DOI: 10.3390/met10010143

[26] Havia, J., Lipiäinen, K., Ahola, A., & Björk, T. (2024). Fatigue design of stress relief grooves to prevent weld root fatigue in butt-welded cast steel to ultra-high-strength steel joints. *Welding in the world*, *68*, 1–14. DOI: 10.1007/s40194-024-01797-3

[27] Nandagopal, K., & Kailasanathan, C. (2016). Analysis of mechanical properties and optimization of gas tungsten Arc welding (GTAW) parameters on dissimilar metal titanium (6Al4V) and aluminium 7075 by Taguchi and ANOVA techniques. *Journal of alloys and compounds*, *682*, 503–516. DOI: 10.1016/j.jallcom.2016.05.006

[28] Kumar, S., Singh, P. K., & D Patel, S. B. P. (2017). Optimization of welding parameters of GTAW using response surface methodology. *Scientific bulletin series-d*, *79*(3), 119–132. http://www.scientificbulletin.upb.ro/rev_docs_arhiva/rezb55_984682.pdf

[29] Kumar, S., Singh, P. K., Patel, D., & Prasad, S. B. (2019). Experimental investigation and optimization of welding parameters on tig welding of stainless steel aisi 304 plates. *Innovation in materials science and engineering: proceedings of icemit 2017*, (pp. 91–102). DOI: 10.1007/978-981-13-2944-9_10

[30] Khalid, M. (2019). Process parameters optimization of tungsten inert gas welding by taguchi method. *2019 advances in science and engineering technology international conferences (ASET)*. (pp. 1–5). DOI: 10.1109/ICASET.2019.8714210

[31] Dewangan, S., Mohapatra, S. K., & Sharma, A. (2020). An assessment into mechanical properties and microstructural behavior of TIG welded Ti-6Al-4V titanium alloy. *Grey systems: theory and application*, *10*(3), 281–292. DOI: 10.1108/GS-11-2019-0052

[32] Miao, Y., Ma, Z., Yang, X., Liu, J., & Han, D. (2018). Experimental study on microstructure and mechanical properties of AA6061/Ti-6Al-4V joints made by bypass-current MIG welding-brazing. *Journal of materials processing technology*, *260*, 104–111. DOI: 10.1016/j.jmatprotec.2018.05.019

[33] Zhang, Y., Huang, J., Ye, Z., & Cheng, Z. (2017). An investigation on butt joints of Ti6Al4V and 5A06 using MIG/TIG double-side arc welding-brazing. *Journal of manufacturing processes*, *27*, 221–225. DOI: 10.1016/j.jmapro.2017.05.010

[34] Sen, R., Choudhury, S. P., Kumar, R., & Panda, A. (2018). A comprehensive review on the feasibility study of metal inert gas welding. *Materials today: proceedings*, *5*(9), 17792–17801. DOI: 10.1016/j.matpr.2018.06.104

[35] Arunkumar, S. P., Prabha, C., Saminathan, R., Khamaj, J. A., Viswanath, M., Ivan, C. K. P., … Kumar, P. M. (2022). Taguchi optimization of metal inert gas (MIG) welding parameters to withstand high impact load for dissimilar weld joints. *Materials today: proceedings*, *56*, 1411–1417. DOI: 10.1016/j.matpr.2021.11.619

[36] Madavi, K. R., Jogi, B. F., & Lohar, G. S. (2022). Metal inert gas (MIG) welding process: A study of effect of welding parameters. *Materials today: proceedings*, *51*, 690–698. DOI: 10.1016/j.matpr.2021.06.206

[37] Cheepu, M., Venkateswarlu, D., Rao, P. N., Kumaran, S. S., & Srinivasan, N. (2019). The influence of gas tungsten arc welding parameters on mechanical and microstructure properties of the tc4 titanium alloy. *Materials science forum* (pp. 895–900). DOI: 10.4028/www.scientific.net/MSF.969.895

[38] Szwajka, K., Zielińska-Szwajka, J., & Trzepieciński, T. (2024). The influence of the shielding-gas flow rate on the mechanical properties of TIG-welded butt joints of commercially pure grade 1 titanium. *Materials*, *17*(5), 1217. DOI: 10.3390/ma17051217

[39] Brykov, M. N., Petryshynets, I., Džupon, M., Kalinin, Y. A., Efremenko, V. G., Makarenko, N. A., … Kováč, F. (2020). Microstructure and properties of heat affected zone in high-carbon steel after welding with fast cooling in water. *Materials*, *13*(22), 5059. DOI: 10.3390/ma13225059

[40] Barriobero-Vila, P., Requena, G., Warchomicka, F., Stark, A., Schell, N., & Buslaps, T. (2015). Phase transformation kinetics during continuous heating of a $β$-quenched Ti-10V-2Fe-3Al alloy. *Journal of materials science*, *50*, 1412–1426. DOI: 10.1007/s10853-014-8701-6

[41] Bak, G. R., Won, J. W., Choe, H.-J., Park, C. H., & Hyun, Y.-T. (2019). Effect of iron content on β→α phase transformation behavior of Ti-5Al-xFe (x=1, 2.5, 4) alloys during continuous cooling. *Journal of materials research and technology*, *8*(3), 2887–2897. DOI: 10.1016/j.jmrt.2019.02.020

[42] Ogunmefun, O. A., Bayode, B. L., Jamiru, T., & Olubambi, P. A. (2023). A critical review of dispersion strengthened titanium alloy fabricated through spark plasma sintering techniques. *Journal of alloys and compounds*, *960*, 170407. DOI: 10.1016/j.jallcom.2023.170407

[43] Williams, J. C., & Boyer, R. R. (2020). Opportunities and issues in the application of titanium alloys for aerospace components. *Metals*, *10*(6), 705. DOI: 10.3390/met10060705

[44] Thesiya, D., Dave, J., Rajurkar, A., & Prajapati, V. (2015). Study on influence of edm process parameters during machining of Ti-6Al-4V. *Journal of manufacturing technology research*, *7*(1/2), 53. https://encr.pw/VVfQ8

[45] Elshaer, R. N., & Ibrahim, K. M. (2022). Applications of titanium alloys in aerospace manufacturing: a brief review. *The bulletin tabbin institute for metallurgical studies (TIMS)*, *111*(1), 60–69. DOI: 10.21608/tims.2023.174504.1007

[46] Tomchik, G., & Dunder, T. G. (2006). Overview of titanium applications on advanced commercial transports. *AeroMat conference, unpublished research*. https://l1nq.com/TxPWN

[47] Moiseyev, V. N. (2005). *Titanium alloys: russian aircraft and aerospace applications*. CRC press. DOI: 10.1201/9781420037678

[48] Anil Kumar, V., Gupta, R. K., Prasad, M., & Narayana Murty, S. V. S. (2021). Recent advances in processing of titanium alloys and titanium aluminides for space applications: A review. *Journal of materials research*, *36*, 689–716. DOI: 10.1557/s43578-021-00104-w

[49] Antunes, R. A., Salvador, C. A. F., & Oliveira, M. C. L. de. (2018). Materials selection of optimized titanium alloys for aircraft applications. *Materials research*, *21*, e20170979. DOI: 10.1590/1980-5373-MR-2017-0979

[50] Veiga, C., Davim, J. P., Loureiro, A. J. R., & others. (2012). Properties and applications of titanium alloys: a brief review. *Reviews on advanced materials science*, *32*(2), 133–148.

[51] Cotton, J. D., Briggs, R. D., Boyer, R. R., Tamirisakandala, S., Russo, P., Shchetnikov, N., & Fanning, J. C. (2015). State of the art in beta titanium alloys for airframe applications. *Jom*, *67*(6), 1281–1303. DOI: 10.1007/s11837-015-1442-4

[52] Tiwary, A., Kumar, R., & Chohan, J. S. (2022). A review on characteristics of composite and advanced materials used for aerospace applications. *Materials today: proceedings*, *51*, 865–870. DOI: 10.1016/j.matpr.2021.06.276

[53] Khatarkar, S., Rao, D. J., & Jha, S. K. (2021). Indigenous development of titanium compressor blade for turbofan engine. *Journal of aerospace sciences and technologies*, 250–266. https://www.researchgate.net/publication/283863116

[54] Hémery, S., & Villechaise, P. (2017). Influence of $β$ anisotropy on deformation processes operating in Ti-5Al-5Mo-5V-3Cr at room temperature. *Acta materialia*, *141*, 285–293. DOI: 10.1016/j.actamat.2017.09.023

[55] Huet, A., Naït Ali, A., Giroud, T., Villechaise, P., & Hémery, S. (2022). Onset of plastic deformation and strain localization in relation to β phase in metastable β and dual phase Ti alloys. *Acta materialia*, *240*, 118348. DOI: 10.1016/j.actamat.2022.118348

[56] Zhang, X., Mei, Y., Lv, Y., Chen, C., & Zhou, K. (2018). Anisotropy of the microstructure and tensile properties in Ti-5Al-5Mo-5V-1Cr-1Fe near β titanium alloy during hot rolling and heat treatment. *Metals*, *8*(11), 904. DOI: 10.3390/met8110904

[57] Kumar, V. A., Gupta, R. K., Chakravadhanula, V. S. K., Rao, A. G., Prasad, M., & Murty, S. (2019). Effect of test temperature on tensile behavior of Ti-5Al-5V-2Mo-1Cr-1Fe ($α$+ $β$) titanium alloy with initial microstructures in hot forged and heat treated conditions. *Metallurgical and materials transactions a*, *50*, 2702–2719. DOI: 10.1007/s11661-019-05207-y

[58] Lhadi, S., Chini, M. R., Richeton, T., Gey, N., Germain, L., & Berbenni, S. (2018). Micromechanical modeling of the elasto-viscoplastic behavior and incompatibility stresses of $β$-Ti alloys. *Materials*, *11*(7), 1227. DOI: 10.3390/ma11071227

[59] Lhadi, S., raj purohit Purushottam raj purohit, R., Richeton, T., Gey, N., Berbenni, S., Perroud, O., & Germain, L. (2020). Elasto-viscoplastic tensile behavior of as-forged Ti-1023 alloy: experiments and micromechanical modeling. *Materials science and engineering: a*, *787*, 139491. DOI: 10.1016/j.msea.2020.139491

[60] Li, P., Chen, S., Dong, H., Ji, H., Li, Y., Guo, X., … Han, X. (2020). Interfacial microstructure and mechanical properties of dissimilar aluminum/steel joint fabricated via refilled friction stir spot welding. *Journal of manufacturing processes*, *49*, 385–396. DOI: 10.1016/j.jmapro.2019.09.047

[61] Dong, R., Zhang, X., Li, C., Zhao, Y., Tian, J., Wu, L., & Hou, H. (2022). Correlation between the mechanical properties and the <110> texture in a hot-rolled near $β$ titanium alloy. *Journal of materials science & technology*, *97*, 165–168. https://api.semanticscholar.org/CorpusID:237652493

[62] Wassermann, G., & Grewen, J. (1962). Textures of metallic materials. *Springer-verlag, German, Berlin*, 181. DOI: 10.1007/978-3-662-13128-2

[63] Engler, O., Randle, V., & others. (2003). *Introduction to texture analysis: macrotexture, microtexture, and orientation mapping*. https://digital.library.tu.ac.th/tu_dc/frontend/Info/item/dc:10625

[64] Suwas, S., & Ray, R. K. (2014). *Crystallographic texture of materials*. Springer. DOI: 10.1007/978-1-4471-6314-5

[65] Banerjee, D., & Williams, J. C. (2013). Perspectives on titanium science and technology. *Acta materialia*, *61*(3), 844–879. DOI: 10.1016/j.actamat.2012.10.043

[66] Bewlay, B. P., Nag, S., Suzuki, A., & Weimer, M. J. (2016). TiAl alloys in commercial aircraft engines. *Materials at high temperatures*, *33*(4–5), 549–559. DOI: 10.1080/09603409.2016.1183068

[67] Nie, X., He, W., Cao, Z., Song, J., Li, X., Pang, Z., & Yan, X. (2021). Experimental study and fatigue life prediction on high cycle fatigue performance of laser-peened TC4 titanium alloy. *Materials science and engineering: a*, *822*, 141658. DOI: 10.1016/j.msea.2021.141658

[68] Wang, Y., Zhu, Z., Sha, A., & Hao, W. (2023). Low cycle fatigue life prediction of titanium alloy using genetic algorithm-optimized BP artificial neural network. *International journal of fatigue*, *172*, 107609. DOI: 10.1016/j.ijfatigue.2023.107609

[69] Guo, Y., Wang, S., & Liu, G. (2024). Creep-fatigue life prediction of a titanium alloy deep-sea submersible using a continuum damage mechanics-informed BP neural network model. *Ocean engineering*, *311*, 118826. DOI: 10.1016/j.oceaneng.2024.118826

[70] Jinlong, W., Wenjie, P., Jing, Y., Jingsi, W., Mingchao, D., & Yuanliang, Z. (2021). Effect of surface roughness on the fatigue failure and evaluation of TC17 titanium alloy. *Materials science and technology*, *37*(3), 301–313. DOI: 10.1080/02670836.2021.1885777

[71] Tukahirwa, G., & Wandera, C. (2023). Influence of process parameters in gas-metal arc welding (GMAW) of carbon steels. In *Welding-materials, fabrication processes, and industry 5.0*. IntechOpen. DOI: 10.5772/intechopen.1002730

[72] Ikpe, A. E., Ikechukwu, O., & Ikpe, E. (2017). Effects of arc voltage and welding current on the arc length of tungsten inert gas welding (TIG). *International journal of engineering and technology (IJET)*, *3*(4), 213-221. https://hdl.handle.net/11363/556

[73] Owunna, I. B., Ikpe, A. E., & Ohwoekevwo, J. U. (2022). Application of SEM/EDS in fractographic investigation of TIG welded AISI 1020 fusion zones at distinct welding current steps. *ARID zone journal of engineering, technology & environment*, *18*(2), 1596–2644. https://www.ajol.info/index.php/azojete/article/view/239702/226560

[74] Hölscher, L. V., Hassel, T., & Maier, H. J. (2022). Detection of the contact tube to working distance in wire and arc additive manufacturing. *The international journal of advanced manufacturing technology*, *120*(1), 989–999. DOI: 10.1007/s00170-022-08805-0

[75] Sato, Y., Ogino, Y., & Sano, T. (2024). Process parameters and their effect on metal transfer in gas metal arc welding: a driving force perspective. *Welding in the world*, *68*(4), 905–913. DOI: 10.1007/s40194-023-01670-9

[76] Quazi, M. M., Ishak, M., Fazal, M. A., Arslan, A., Rubaiee, S., Qaban, A., … Manladan, S. M. (2020). Current research and development status of dissimilar materials laser welding of titanium and its alloys. *Optics & laser technology*, *126*, 106090. DOI: 10.1016/j.optlastec.2020.106090

[77] Messler Jr, R. W. (2019). *A Practical guide to welding solutions: overcoming technical and material-specific issues*. John Wiley & Sons. https://books.google.com/books?id=VvaFDwAAQBAJ&printsec=frontcover#v=onepage&q&f=false

[78] Tolvanen, S. (2018). *Welding of Ti-6Al-4V: influence of welding process and alloy composition on microstructure and properties*. [Thesis]. https://research.chalmers.se/en/publication/504433

[79] Song, Z., Wu, S., Hu, Y., Kang, G., Fu, Y., & Xiao, T. (2018). The influence of metallurgical pores on fatigue behaviors of fusion welded AA7020 joints. *Acta metallurgica sinica*, *54*(8), 1131–1140. DOI: 10.11900/0412.1961.2017.00448

[80] Yi, H. J., Lee, Y. J., & Lee, K. O. (2016). TIG dressing effects on weld pores and pore cracking of titanium weldments. *Metals*, *6*(10), 243. DOI: 10.3390/met6100243

[81] Sen, M., & Kurt, M. (2022). Laser and TIG welding of additive manufactured Ti-6Al-4V parts. *Materials testing*, *64*(5), 656–666. DOI: 10.1515/mt-2021-2165

[82] Chen, S., Luo, S., Yu, H., Geng, H., Xu, G., Li, R., & Tian, Y. (2020). Effect of beam defocusing on porosity formation in laser-MIG hybrid welded TA2 titanium alloy joints. *Journal of manufacturing processes*, *58*, 1221–1231. DOI: 10.1016/j.jmapro.2020.09.026

[83] Junaid, M., Khan, F. N., Rahman, K., & Baig, M. N. (2017). Effect of laser welding process on the microstructure, mechanical properties and residual stresses in Ti-5Al-2.5 Sn alloy. *Optics & laser technology*, *97*, 405–419. DOI: 10.1016/j.optlastec.2017.07.010

[84] J. X. Zhang, Y. X., & Gong, S. L. (2005). Residual welding stresses in laser beam and tungsten inert gas weldments of titanium alloy. *Science and technology of welding and joining*, *10*(6), 643–646. DOI: 10.1179/174329305X48374

[85] Łagoda, T., & Głowacka, K. (2020). Fatigue life prediction of welded joints from nominal system to fracture mechanics. *International journal of fatigue*, *137*, 105647. DOI: 10.1016/j.ijfatigue.2020.105647

[86] Zhan, Y., Zhang, E., Ge, Y., & Liu, C. (2018). Residual stress in laser welding of TC4 titanium alloy based on ultrasonic laser technology. *Applied sciences*, *8*(10), 1997. DOI: 10.3390/app8101997

[87] Xu, L. Y., Zhu, J., Jing, H. Y., Zhao, L., Lv, X. Q., & Han, Y. D. (2016). Effects of deep cryogenic treatment on the residual stress and mechanical properties of electron-beam-welded Ti-6Al-4V joints. *Materials science and engineering: a*, *673*, 503–510. DOI: 10.1016/j.msea.2016.07.101

[88] Liu, J., Zheng, J., Fu, B., Bu, L., Li, R., & Liu, S. (2023). Thermo-mechanical study of TIG welding of Ti-6Al-4V for residual stresses considering solid state phase transformation. *Metals*, *13*(5), 1001. DOI: 10.3390/met13051001

[89] Li, Y., Wu, A., Li, Q., Zhao, Y., Zhu, R., & Wang, G. (2019). Effects of welding parameters on weld shape and residual stresses in electron beam welded Ti2AlNb alloy joints. *Transactions of nonferrous metals society of china*, *29*(1), 67–76. DOI: 10.1016/S1003-6326(18)64916-7

[90] Wang, L., & Qian, X. (2022). Welding residual stresses and their relaxation under cyclic loading in welded S550 steel plates. *International journal of fatigue*, *162*, 106992. DOI: 10.1016/j.ijfatigue.2022.106992

[91] Wang, L., & Qian, X. (2024). Effects of pre-tension and fatigue loadings on the evolution of welding residual stresses in welded plates. *Engineering structures*, *301*, 117272. DOI: 10.1016/j.engstruct.2023.117272

[92] Hemmesi, K., Mallet, P., & Farajian, M. (2020). Numerical evaluation of surface welding residual stress behavior under multiaxial mechanical loading and experimental validations. *International journal of mechanical sciences*, *168*(15), 105127. DOI: 10.1016/j.ijmecsci.2019.105127